Supplementary Materials for

Atomic model for the dimeric F_O region of mitochondrial ATP synthase

Hui Guo, Stephanie A. Bueler, and John L. Rubinstein
correspondence to: john.rubinstein@utoronto.ca

This PDF file includes:

Materials and Methods
Supplementary Text
Figs. S1 to S4
Table S1

Materials and Methods

Yeast strain construction, growth, and protein purification

Yeast strain SABY93 was prepared from haploid strain W303-1A by inserting DNA sequence for a 3×FLAG tag followed by a *URA3* marker at the 3′ end of the *ATP4* gene (subunit b) as described previously (*36*). Yeast were cultured in a 11 L Microferm fermentor (New Brunswick Scientific) in YPG medium and mitochondria were isolated by bead-beating (*37*). All protein preparation steps were performed at 4 ºC. For purification of the F_O complex, mitochondria were washed with phosphate buffer (50 mM sodium phosphate pH 9.0, 5 mM ε-amino-n-caproic acid, 5 mM p-aminobenzamidine, 1 mM PMSF) for 30 min and membranes collected by centrifugation at 184,000 g for 30 min. Submitochondrial particles were prepared by suspending membranes in SMP Buffer (50 mM Tris-HCl pH 7.4, 250 mM sucrose, 5 mM ε-amino-n-caproic acid, 5 mM p-aminobenzamidine, 1 mM PMSF) and soliciting on ice with a Misonix Sonicator 3000 at ~50 W with cycles of 1 s on and 10 s off for a total of 22 min. F_1 regions were stripped from membranes by addition of sodium bromide to 3 M followed by mixing for 10 min (*19*). Stripped membranes were collected as the floating layer after centrifugation at 105,000 g for 30 min and diluted 1:4 with SMP buffer. Membranes were then collected by centrifugation at 184,000 g for 30 min, suspended in purification buffer (50 mM Tris-HCl pH 7.4, 300 mM NaCl, 10 % [w/v] glycerol, 5 mM ε-amino-n-caproic acid, 5 mM p-aminobenzamidine, 1 mM PMSF, 0.02 % [w/v] glyco-diosgenin [GDN]) and solubilized by addition of GDN to 1 % (w/v) and mixing for 2 h. Insoluble material was removed by centrifugation at 184,000 g for 20 min and solubilized membranes were loaded onto a column of 500 µL M2 agarose beads (Sigma) pre-equilibrated with purification buffer, washed with five column volumes of purification buffer, and eluted with four column volumes of purification buffer containing 150 µg/ml 3×FLAG peptide. Purified protein was concentrated to ~5 mg/ml with a 100 kDa MWCO Vivaspin 500 centrifuged concentrator (Sartorius) prior to storage at -80 ºC. Intact dimeric ATP synthase was purified the same way as the F_O complex but without the sodium bromide step.

Cryo-EM and image analysis

Immediately prior to grid freezing, glycerol was removed from samples with a Zeba spin desalting column (ThermoFisher scientific). Purified F_O dimers (2.5 µl) were applied to homemade nanofabricated EM grids (*38*) consisting of a holey layer of gold on carbon (*39*) that had been glow-discharged in air for 2 min. EM grids were then blotted in a FEI Vitrobot for 26 s with ~100 % RH at 4 °C before freezing in a liquid ethane/propane mixture (*40*). Specimens were optimized and a preliminary dataset acquired with a FEI Tecnai F20 electron microscope operating at 200 kV and equipped with a Gatan K2 Summit camera. The best regions of the specimen often formed noticeable ice thickness gradients. Micrographs were recorded in counting mode as 15 s movies at 2 frames per second with an exposure rate of ~5 electrons/pixel/second, and a calibrated pixel size of 1.45 Å. High-resolution data were collected at the New York Structural Biology Centre (NYSBC) with a FEI Titan Krios electron microscope (Krios 3) operated at 300 kV and automated with *Leginon* (*41*). Zero-loss energy-filtered movies were recorded with a Gatan Quantum energy filter (slit width of 20 eV) and K2 Summit camera. The camera

was used in counting mode with movies collected for 10 s at 5 frames per second, an exposure rate of ~8 electrons/pixel/second, and a calibrated pixel size of 1.06 Å. While collecting data in super-resolution mode provides slightly improved detective quantum efficiency at high resolution compared to counting mode, we and others have found this advantage to be small and outweighed by faster image acquisition in counting mode.

From the F20 microscope, 793 movies of the F_O complex were collected. Frames were aligned and averaged with *alignframes_lmbfgs* (*42*) and 239,159 single particle images were selected from the aligned frames with *RELION* 1.4 (*43*). Image CTF parameters were estimated with *CTFFIND4* (*44*). Individual particle motion was corrected with *alignparts_lmbfgs* (*42*) and particle images and CTF parameters were adjusted for a previously measured anisotropic magnification in the F20 microscope (*45*). The resulting particle images were used for *ab initio* 3D classification with *cryoSPARC* (*46*) and a single 3D class, containing 172,064 particle images was refined to 4.4 Å resolution with C2 symmetry (5.0 Å without symmetry). For intact ATP synthase dimers, 626 movies were collected from which 79,942 particle images from a single 3D class gave a map at 7.4 Å resolution with C2 symmetry. From the Titan Krios microscope 3,023 movies of F_O complex were collected, from which 2,432 movies exhibiting good particle distributions and image power spectra were selected for further processing. These movies were initially processed at NYSBC with *MotionCor2* (*47*) to correct stage drift and beam induced motion. Image brightness gradients from varying ice thickness, emphasized by the energy filter, interfered with automatic particle selection in *RELION* and were removed for particle selection by high-pass filtering with *imagicfilter_fftw* (https://sites.google.com/site/rubinsteingroup/image-stack-utilities). Following the same strategy as with the F20 microscope, 470,036 particle images were selected and 166,263 ultimately used in *cryoSPARC* to produce a 3D map at 4.5 Å resolution. Reprocessing the movies with *alignframes_lmbfgs* and *alignparts_lmbfgs* allowed for selection of 446,259 particle images, from which 238,848 were used to produce a 3.6 Å resolution map with C2 symmetry enforced. Map refinement without enforcing symmetry produced a nearly indistinguishable map at 3.7 Å resolution. This improvement in resolution when using *alignparts_lmbfgs* instead of *MotionCor2* may have been due to anisotropic movement in specimens arising from the ice thickness gradients (Fig. S1B). All Fourier shell correlation (FSC) curves were calculated with independently refined half-maps and resolution was assessed at the 0.143 criterion with correction for the effects of masking maps. Local resolution was estimated with *cryoSPARC*.

Model building/computation

The initial model for subunit c was from PDB 5BPS. Models for all other subunits were built manually in *Coot* (*48*). Final models were built with successive rounds of manual model building in *Coot* and real space refinement in *Phenix* (*49*) and gave an *EMRinger* score of 2.58 for the entire model (*50*), which is better than typical score of 1.0, or the good score of 2.0, for a 3.5 Å resolution map. 91.54, 8.33, and 0.14 % of residues were in preferred, allowed, and disallowed regions of the Ramachandran plot, respectively, with no Ramachandran outliers in the α-helical regions of the model. All figures were rendered with UCSF Chimera (*51*). To evaluate possible over-fitting during atomic model refinement the FSC_{work} and FSC_{test} between the model and the two

independent density maps, each from half of the dataset, were calculated as described (*52*). Briefly, random coordinate shifts of up to 0.5 Å were applied to the refined model with the shake function in *Phenix*. The shaken model was refined against one of the independent half maps produced from half of the data during map calculation in *cryoSPARC*. This refined model was converted to a density map with the molmap command in *USCF Chimera* and the FSC between this density and the half map used for the refinement (FSC_{work}), as well as the half map that was not used for the refinement (FSC_{test}), were calculated and compared (Fig. S1D).

Supplementary Text

Subunit assigments

The model for the *S. cerevisiae* F_O complex presented here identifies several of the transmembrane α-helical segments differently from analysis of lower-resolution cryo-EM maps. These identities were established based on the following evidence.

Subunit b: The assignment of density as the N-terminal α-helix of subunit b was enabled by the presence of strong density connecting it to the rest of subunit b, particularly in the unsharpened version of the map.

Subunit i/j: The density identified as subunit i/j showed clear side chains in a trans-membrane α-helix. Only the sequence corresponding to subunit i/j could be fit into this density, with Y13, W14, P15, F16, F17, Y24, and Y25 filling bulky side chain protrusions in the density and G20 of subunit i/j also fitting the density well.

Subunit f: Only the sequence of subunit f could be fit into the transmembrane α-helical density subsequently identified as subunit f. In particular, the density matched bulky side chain residues W67, H68, F69, F76, and Y78 from the subunit f sequence as well as G72 and G77.

Subunit e: The primary sequence of subunit e suggests that it has an N-terminal hydrophobic transmembrane α-helix (protein sequence NVLRYSALGLGLFFGFRNDMIL) that experiments have shown is followed by a soluble region that extends into the mitochondrial IMS (*53*). The approximate position of subunit e and g are also known from comparison of ATP synthase structures with and without subunits e and g present (*13*, *11*). Therefore, subunit e was built as poly-alanine into the map density with an N-terminal transmembrane α-helix followed by an IMS α-helix, adjacent to the position of the density identified as subunit g.

Subunit g: Subunit g was identified because its length corresponds to the fully connected α-helices observed in the unsharpened map, the presence of a C-terminal transmembrane α-helix, and N-terminal soluble domain located on the matrix side of the membrane (*54*). Also, subunit g and subunit e are known to interact via a GXXXG motif (*26*, *27*), which also supports our assignment for both subunits.

Subunit k: By elimination, the density identified as subunit k resolved amino acid side chain density in the transmembrane α-helix and could only correspond to the missing subunits k or l. However, only the assignment to subunit k could accommodate residues Y5, H6, F7, G9, P13, P14, H15. Bulky side chain residues from subunit l could not be fit into the density.

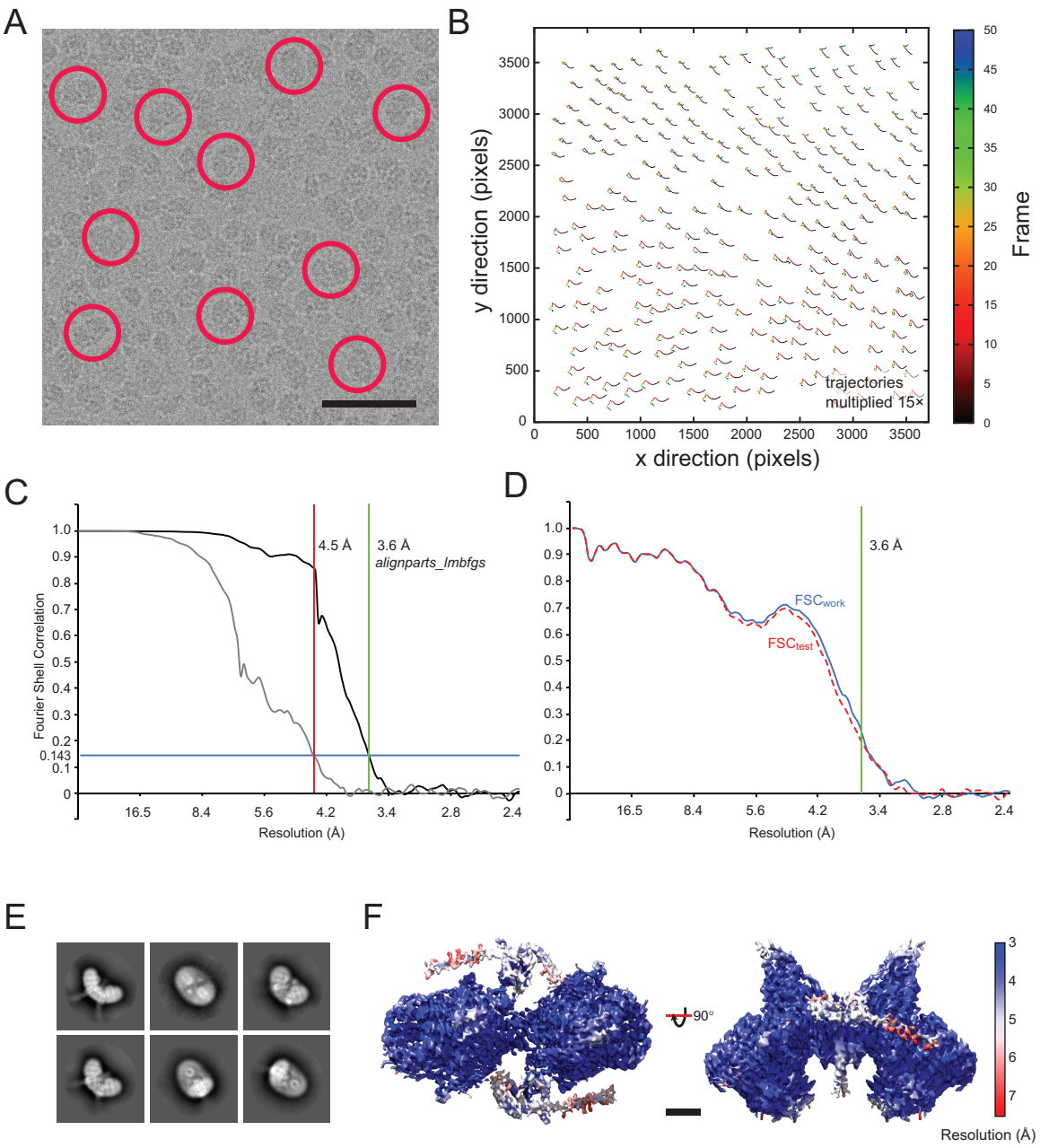

Fig. S1.

Cryo-EM and validation. A, Region of a micrograph, with example protein particles circled in red. Scale bar, 500 Å. **B,** Example trajectories showing anisotropic beam-induced movement of specimen from *alignparts_lmbfgs*. **C,** Fourier shell correlation (FSC) curve corrected for the effects of masking for 300 kV data processed at NRAMM with *MotionCor2* (grey) and *alignparts_lmbfgs* (black). **D**, Comparison of FSC curves for the model with both half maps after refinement of the model against one half map to give FSC_{work} and FSC_{test} (*52*). **E,** 2-D class averages from 200 kV data showing different views of the F_O complex. **F,** Estimation of local resolution in the map. Scale bar, 25 Å.

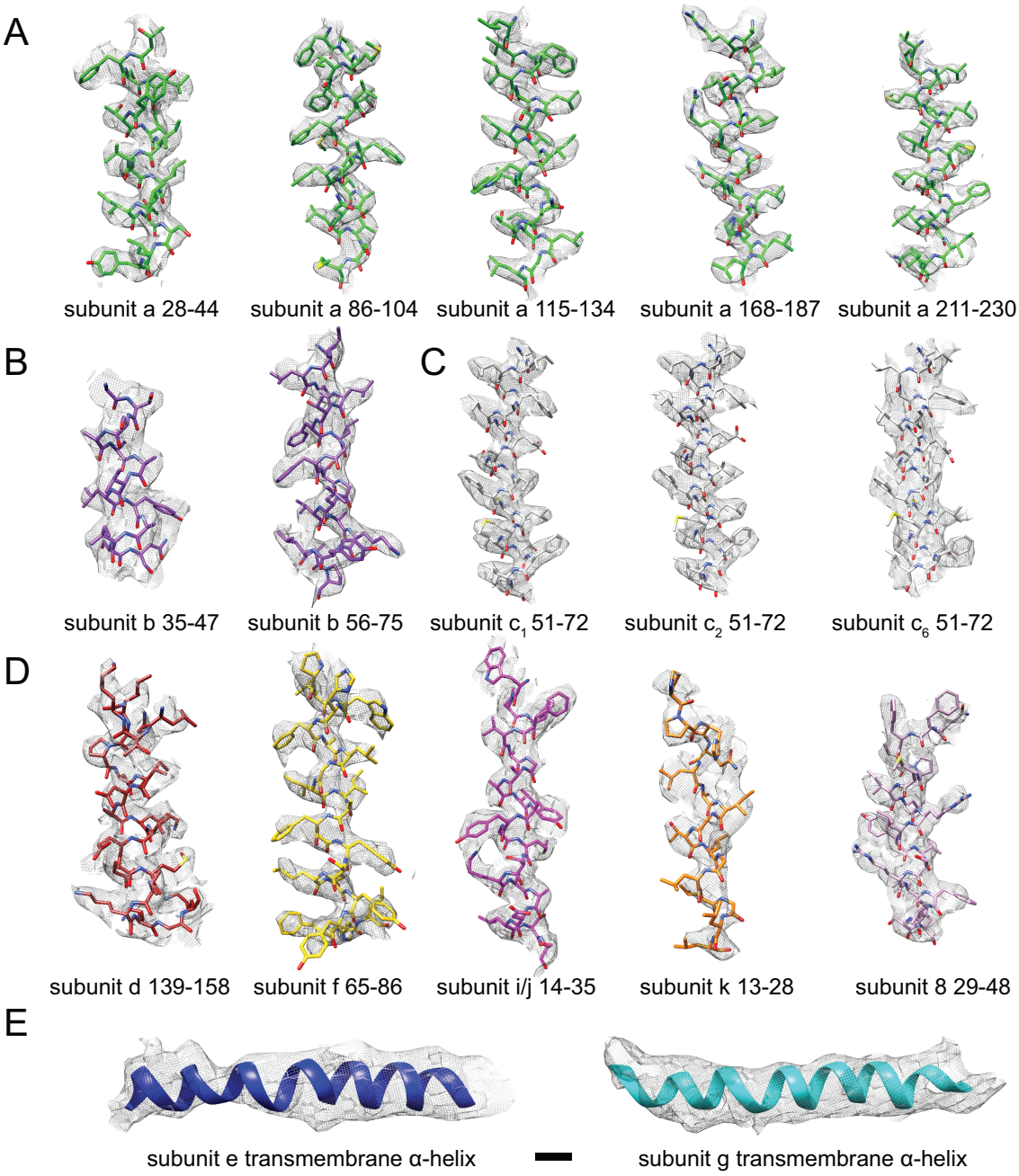

Fig. S2
Examples of atomic models from subunits built in the experimental cryo-EM map.
Scale bar, 5 Å.

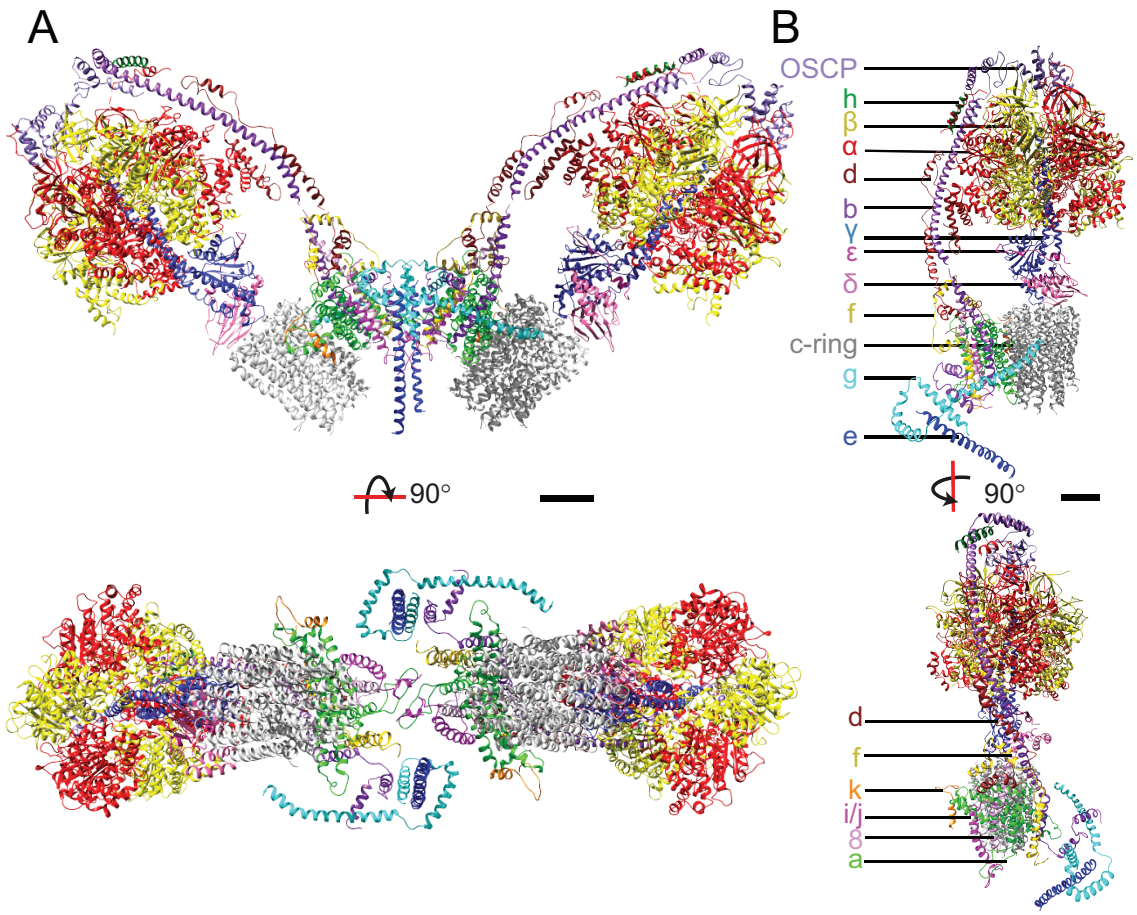

Fig. S3

Mosaic model of the ATP synthase. Nearly complete atomic models for the ATP synthase dimer (**A**) and monomer (**B**) built by combining the F_O model with models for subunits $\alpha_3\beta_3\gamma\delta\varepsilon$ from *S. cerevisiae* (PDB ID 2XOK) and the N terminus of subunit α from *P. angusta* (PDB ID 5LQZ). Subunits OSCP, b, and d are homology models and subunit h was built as poly-alanine from the *P. angusta* structure. The N-terminal region of subunit f was built as poly-alanine into the *P. angusta* cryo-EM map (EMD4102). Scale bars, 25 Å.

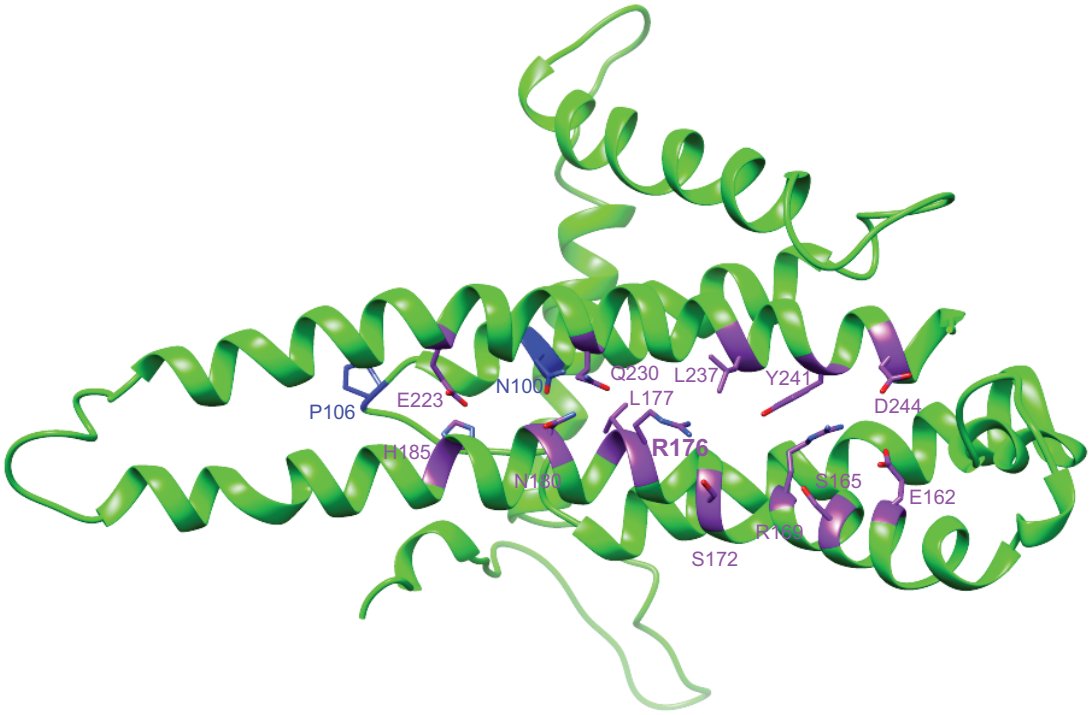

Fig. S4

Conserved residues in subunit a. Conserved residues are from Ref (*9*). Residues on transmembrane α-helices 3 and 4 are in blue and residues on transmembrane α-helices 5 and 6 are in purple. Scale bar, 25 Å.

Table S1.

Cryo-EM data acquisition, processing, and atomic model statistics.

Data Collection	
Electron Microscope	FEI Titan Krios
Camera	Quantum/K2 Summit
Voltage	300 kV
Nominal Magnification	130,000×
Calibrated physical pixel size	1.06 Å
Total exposure	71 electrons/Å^2
Exposure rate	8 electrons/pixel/s
Number of frames	50
Defocus range	0.5 to 3.5 μm
Image Processing	
Motion correction software	*alignparts_lmbfgs*
CTF estimation software	*CTFFIND4*
Particle selection software	*Relion* 1.4
Micrographs used	2,432
Particles selected	446,259
3D map classification and refinement software	*cryoSPARC*
Particles contributing to final map	238,848
Applied symmetry	C2
Applied B-factor	129 Å^2
Global resolution (FSC = 0.143)	3.6 Å
Model Building	
Modeling software	*Coot, Phenix*
Number of residues built	2994
RMS (bonds)	0.00 Å
RMS (angles)	0.71°
Ramachandaran outliers	0.14 %
Ramachandran favoured	91.54 %
Clashscore	11.16
MolProbity score	2.07
EMRinger score	2.58